$CaAl_2Si_2$-type Arsenides $RE_{2/3}Zn_2As_2$ (RE = La, Ce, Pr, Nd, Sm)

André T. Nientiedt, Hannes Lincke, Ute Ch. Rodewald, Rainer Pöttgen, and Wolfgang Jeitschko

Institut für Anorganische und Analytische Chemie, Universität Münster, Corrensstraße 30, 48149 Münster, Germany

Reprint requests to R. Pöttgen. E-mail: pottgen@uni-muenster.de

Z. Naturforsch. **2011**, *66b,* 221 – 226; received December 20, 2010

The ternary arsenides $RE_{2/3}Zn_2As_2$ (RE = La, Ce, Pr, Nd, Sm) were synthesized from the elements in NaCl/KCl salt fluxes and were characterized by powder X-ray diffraction. The $Ce_{2/3}Zn_2As_2$ structure was refined on the basis of single-crystal X-ray diffractometer data: $CaAl_2Si_2$ type, $P\bar{3}m1$, Z = 1, a = 417.17(6), c = 703.7(1) pm, $wR2$ = 0.0353, 211 F^2 values, 11 variables, SOF(Ce) = 62.9(5) %. The zinc and arsenic atoms form a two-dimensional network of edge-sharing $ZnAs_{4/4}$ tetrahedra with Zn–As distances of 253 pm. These covalently bonded $[Zn_2As_2]^{2-}$ layers are separated and charge-balanced by the cerium atoms. Each cerium atom has a slightly distorted octahedral arsenic coordination (Ce–As 302 pm). The defect type of the $RE_{2/3}Zn_2As_2$ arsenides is discussed with respect to isotypic sulfides $RE_{2/3}Cu_2S_2$.

Key words: Arsenides, Rare Earth Compounds, Crystal Structure

Introduction

Among the huge number of ternary intermetallic compounds $RE_xT_yX_z$ (RE = rare earth element, T = transition metal, X = element of the 3rd, 4th, or 5th main group), those with the tetragonal $ThCr_2Si_2$-type structure [1] form one of the largest groups. So far more than 2000 entries are listed in the Pearson data base [2, 3]. These compounds have intensively been studied in the past forty years with respect to their greatly varying physical properties. A recent prominent example is the discovery of superconductivity in potassium-doped $BaFe_2As_2$ [4, 5].

Depending on the electron count and the size of the atoms, for the same composition also the trigonal $CaAl_2Si_2$ type [6] ($\equiv$ Ce_2O_2S [7], a ternary ordered version of La_2O_3) frequently occurs. More than 200 compounds with this atomic arrangement are known. Most of them can be rationalized with an electron-precise description, *e. g.* $Ca^{2+}(Al^{3+})_2(Si^{4-})_2$ or $(Ce^{3+})_2(O^{2-})_2S^{2-}$. Emphasizing the tetrahedral networks of the aluminum and silicon, respectively cerium and oxygen atoms, one can write $Ca^{2+}[Al_2Si_2]^{2-}$ and $[Ce_2O_2]^{2+}S^{2-}$, where the calcium and sulfide atoms separate the tetrahedral layers. The technically most prominent member of the oxide sulfides is europium-doped Y_2O_2S, one of the widely used red phosphors.

Among the pnictides (Pn) with $CaAl_2Si_2$-type structure, those with the divalent alkaline earth elements (AE) and divalent europium and ytterbium also follow an electron-precise description. Most of the experimental work on these phases was carried out in the Mewis group [8, and refs. therein]. When it comes to members with the trivalent rare earth elements, it is more difficult to fulfill the electronic requirements. Formation of the $CaAl_2Si_2$-type structure is possible through substitution of the transition metal component. To give an example, in starting from $AEZn_2Pn_2$ an isotypic compound with a rare earth element is reached *via* substitution of half of the divalent zinc atoms by monovalent copper atoms, leading to the series REZn$Cu Pn_2$ [9, and refs. therein]. Another way out to reduce the valence electron concentration is the formation of defects on the rare earth sites, as realized for the sulfides $Gd_{2/3}Cu_2S_2$ [10] and $Er_{2/3}Cu_2S_2$ [11] and diverse isotypic sulfides, selenides, and tellurides [2, 3].

We have now observed the same defect type for the series of arsenides $RE_{2/3}Zn_2As_2$ (RE = La, Ce, Pr, Nd, Sm). These arsenides were first found as side products during salt flux syntheses of the arsenide $Pr_3Zn_2As_6$ [12] and the arsenide oxides REZnAsO [13, 14]. Well-shaped crystals were then

synthesized from samples with the starting compositions $RE : Zn : As = 1 : 3 : 3$.

Experimental Section

Synthesis

The arsenides $RE_{2/3}Zn_2As_2$ (*RE* = La, Ce, Pr, Nd, Sm) were synthesized in salt fluxes. Starting materials were filings of the rare earth elements (Kelpin and Smart Elements, > 99.9 %), zinc granules or zinc powder (Merck, > 99.9 %), arsenic pieces (Sigma-Aldrich, 99.999 %), NaCl (Merck, > 99.5 %), and KCl (Chempur, 99.9 %). The arsenic was purified by fractional sublimation under vacuum prior to use. First, the sesquioxide As_2O_3 was sublimed with the hot end of the sealed silica tube at 570 K and the other end at r. t. After separation of the cold end (containing the sesquioxide) the tube was sealed again, and the arsenic was sublimed with the hot end of the tube at 870 K. The elemental components (∼ 0.5 g) were weighed in a molar ratio of 1 : 3 : 3 (*RE* : Zn : As), then mixed with *ca.* 2 g of a dried equimolar NaCl/KCl matrix and sealed in evacuated silica tubes. The ampoules were positioned in a muffle furnace, first heated to 770 K for one day, followed by annealing at 1070 K for another 7 d. Finally the ampoules were quenched in air and broken off. The salt matrix was dissolved in hot demineralized water. For crystal growth experiments of the cerium-containing sample, in the final step the sample was cooled to 870 K at a rate of 1 K h^{-1}. The resulting samples consisted of black, platelet- or lath-shaped crystals. The samples are stable in air over months.

EDX data

The $RE_{2/3}Zn_2As_2$ samples were studied by EDX using a Leica 420i scanning electron microscope with CeO_2, REF_3, Zn, InAs, albite (for Na), and KCl as standards for the semi-quantitative measurements. The analyses were in good agreement with the ideal composition. No other impurity elements (especially no sodium, potassium and chlorine incorporation from the flux) were observed.

X-Ray diffraction

The polycrystalline $RE_{2/3}Zn_2As_2$ samples were studied by X-ray powder diffraction on a Guinier camera (equipped with an image plate system Fuji-film, BAS-1800) using Cu$K\alpha_1$ radiation and α-quartz (a = 491.30, c = 540.46 pm) as an internal standard. The hexagonal lattice parameters (Table 1, refs. [15–19]) were deduced from least-squares refinements of the powder data. The correct indexing was ensured by comparison of the experimental patterns to calculated ones [20] using the positional parameters obtained from the structure refinement.

Platelets of $Ce_{2/3}Zn_2As_2$ were additionally cleaned in demineralized water in an ultrasonic bath and finally rinsed with acetone. Well-shaped specimens were glued to quartz fibres using beeswax and were characterized by Laue photographs on a Buerger camera (white molybdenum radiation, image plate technique, Fuji-film, BAS-1800) in order to check their suitability for an intensity data collection. The data set was collected at room temperature by use of an IPDS II diffractometer (graphite-monochromatized MoK_α radiation; oscillation mode). A numerical absorption correction was applied to the data set. All relevant crystallographic data and details of the data collection and evaluation are listed in Table 2.

Table 1. Lattice parameters of ternary arsenides AZn_2As_2 and $A_{2/3}Zn_2As_2$.

Compound	a (pm)	c (pm)	V (nm^3)	Reference
$La_{2/3}Zn_2As_2$	418.0(1)	709.3(1)	0.1073	this work
$Ce_{2/3}Zn_2As_2$	417.4(1)	703.2(1)	0.1061	this work
$Pr_{2/3}Zn_2As_2$	416.6(1)	698.5(2)	0.1050	this work
$Nd_{2/3}Zn_2As_2$	416.2(1)	694.1(2)	0.1041	this work
$Sm_{2/3}Zn_2As_2$	415.4(1)	692.4(2)	0.1035	this work
$EuZn_2As_2$	421.1(1)	718.1(1)	0.1103	[15]
$YbZn_2As_2$	416.0(1)	696.1(1)	0.1043	[15, 16]
$YbZn_2As_2$	415.7	695.4	0.1041	[17]
$CaZn_2As_2$	416.2	701.0	0.1052	[18]
$SrZn_2As_2$	422.3(1)	726.8(1)	0.1123	[19]

Table 2. Crystal data and structure refinement for $Ce_{0.629}Zn_2As_2$, space group $P\bar{3}m1$, Z = 1.

Refined composition	$Ce_{0.629(5)}Zn_2As_2$
Formula weight, g mol^{-1}	368.86
Crystal size, μm^3	10 × 40 × 50
Unit cell dimensions (single crystal data)	
a, pm	417.17(6)
c, pm	703.7(1)
Cell volume, nm^3	0.1061
Calculated density, g cm^{-3}	5.78
$F(000)$, e	163
Absorption coefficient, mm^{-1}	33.1
Transm. ratio (max / min)	0.778 / 0.309
Detector distance, mm	60
Exposure time, min	10
ω range; increment, deg	0 – 180, 1.0
Integr. param. A, B, EMS	13.5; 3.5; 0.012
θ range for data collection, deg.	2.8 – 34.8
Range in *hkl*	±6, ±6, ±11
Total no. reflections	1339
Independent reflections / R_{int}	211 / 0.0370
Reflections with $I \geq 2\sigma(I)$ / R_σ	144 / 0.0765
Data / ref. parameters	211 / 11
$R1$ / $wR2$ for $I \geq 2\sigma(I)$	0.0210 / 0.0344
$R1$ / $wR2$ for all data	0.0366 / 0.0353
Goodness-of-fit on F^2	0.739
Extinction coefficient	0.075(5)
Largest diff. peak / hole, e Å^{-3}	1.76 / −1.63

Structure refinement

Isotypism of the $RE_{2/3}Zn_2As_2$ arsenides with the trigonal $CaAl_2Si_2$-type structure was already evident from the

Table 3. Atomic coordinates and anisotropic displacement parameters (pm^2) for $Ce_{0.629(5)}Zn_2As_2$. U_{eq} is defined as one third of the trace of the orthogonalized U_{ij} tensor. The anisotropic displacement factor exponent takes the form: $-2\pi^2[(ha^*)2U_{11} + \ldots + 2hka^*b^*U_{12}]$. $U_{12} = 1/2U_{11}$; $U_{23} = U_{13} = 0$. The cerium site is occupied only by 62.9(5) %.

Atom	Wyck. site	x	y	z	$U_{11} = U_{22}$	U_{33}	U_{eq}
Ce	1*a*	0	0	0	94(5)	78(6)	89(4)
Zn	2*d*	1/3	2/3	0.6323(1)	93(4)	118(5)	101(3)
As	2*d*	1/3	2/3	0.2595(1)	48(3)	73(4)	56(3)

Table 4. Interatomic distances (pm) in $Ce_{0.629(5)}Zn_2As_2$. All distances shorter than 415 pm are listed. Standard deviations are all equal to or smaller than 0.1 pm.

Ce:	6	As	302.2
	6	Zn	353.5
Zn:	3	As	252.6
	1	As	262.4
	3	Zn	304.5
	3	Ce	353.5
As:	3	Zn	252.6
	1	Zn	262.4
	3	Ce	302.3

Guinier powder patterns. Careful evaluation of the diffractometer data set revealed trigonal symmetry and no further systematic extinctions, in agreement with space group $P\bar{3}m1$. The structural parameters of the prototype $CaAl_2Si_2$ [6] were taken as starting values, and the $Ce_{2/3}Zn_2As_2$ structure was refined with anisotropic displacement parameters for all atoms with SHELXL-97 (full-matrix least-squares on F_o^2) [21]. The refinement readily revealed a too high displacement parameter for the 1*a* cerium site, indicating much lower electron density. In the subsequent cycles the cerium site occupancy factor was refined as a least-squares variable, leading to the composition $Ce_{0.629(5)}Zn_2As_2$ for the investigated crystal. The zinc and arsenic sites were fully occupied within two standard deviations. The atomic parameters and interatomic distances are listed in Tables 3 and 4.

Further details of the crystal structure investigation may be obtained from Fachinformationszentrum Karlsruhe, 76344 Eggenstein-Leopoldshafen, Germany (fax: +49-7247-808-666; e-mail: crysdata@fiz-karlsruhe.de, http://www.fiz-informationsdienste.de/en/DB/icsd/depot_anforderung.html) on quoting the deposition number CSD-422446.

Discussion

The new arsenides $RE_{2/3}Zn_2As_2$ (*RE* = La, Ce, Pr, Nd, Sm) crystallize with the trigonal $CaAl_2Si_2$-type structure, Pearson code *hP*5. As expected from the lanthanoid contraction, the lattice parameters decrease from the lanthanum to the samarium compound. So far, $Sm_{2/3}Zn_2As_2$ is the respective arsenide with the smallest cell volume (Fig. 1).

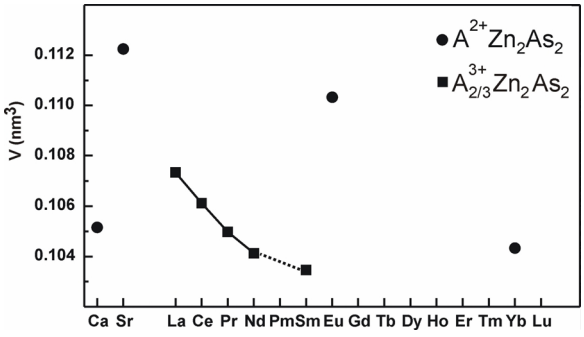

Fig. 1. Plot of the cell volumes of the ternary zinc arsenides AZn_2As_2 and $A_{2/3}Zn_2As_2$ (A = alkaline earth or rare earth element).

The structure consists of a two-dimensional $[Zn_2As_2]$ network (Fig. 2) in which each zinc atom has tetrahedral arsenic coordination at an average Zn–As distance of 255 pm, somewhat longer than the sum of the covalent radii [22] of 246 pm. In ZrCuSiAs-type NdZnAsO [13] and LaZnAsO [14] with a similar network the Zn–As distances of 256 and 257 pm, respectively, are slightly longer. In the body-centered tetragonal modification of Zn_3As_2 [23] the six different kinds of $ZnAs_{4/4}$ tetrahedra have average Zn–As distances varying between 254.8 and 258.2 pm. The connectivity pattern of the $ZnAs_{4/4}$ tetrahedra is similar to the rhombohedral NdZnPO-type structure [13, 24, 25] with $ZnP_{4/4}$ tetrahedra.

The covalently bonded $[Zn_2As_2]$ network is charge-balanced and separated by the cerium atoms, which is the decisive issue concerning the cations. With divalent Ca^{2+}, Sr^{2+}, Eu^{2+}, and Yb^{2+} one obtains an electron-precise description $A^{2+}Zn^{2+}Zn^{2+}As^{3-}As^{3-}$ in agreement with the Zintl concept. This scheme, however, is already violated for $YbZn_2As_2$ [15], which reveals intermediate ytterbium valence in the magnetic susceptibility measurements. In view of the electron precise description of the $[Zn_2As_2]^{2-}$ network, where one cannot account for additional electron density, a way out is the creation of cerium defects, as observed for $Ce_{0.629}Zn_2As_2$ described herein. Data on the ytterbium occupancy, however, have not been reported. The reported slightly lower experimental density of $YbZn_2As_2$ [15] might be a hint for such vacancies.

The almost exact 2/3 occupancy of the rare earth site calls for an ordered vacancy model, where every third rare earth position in the close-packed arrangement is unoccupied. The reciprocal space of the $Ce_{0.629}Zn_2As_2$ data set was therefore carefully studied. In Fig. 3 we

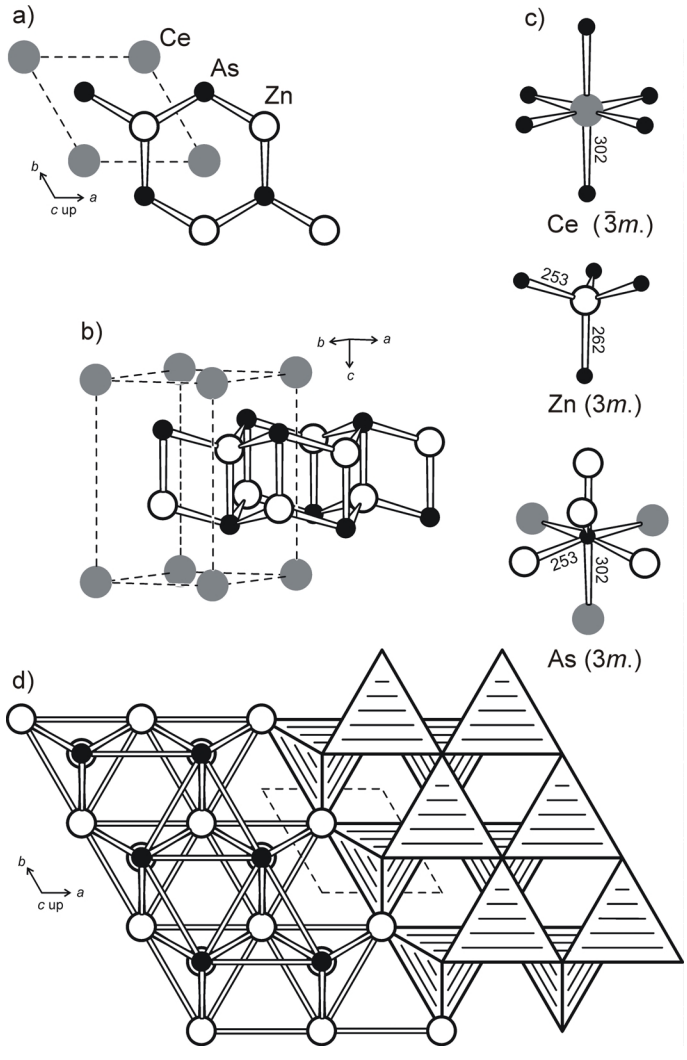

Fig. 2. The crystal structure of $Ce_{2/3}Zn_2As_2$. Cerium. zinc and arsenic atoms are drawn as medium grey, black open and filled circles, respectively. (a) Projection of the structure onto the *xy* plane; (b) view of the $Ce_{2/3}Zn_2As_2$ structure approximately along [110] with an emphasis of the 2D $[Zn_2As_2]$ network; (c) coordination, site symmetry and selected interatomic distances; (d) cutout of the network of edge-sharing $ZnAs_{4/4}$ tetrahedra.

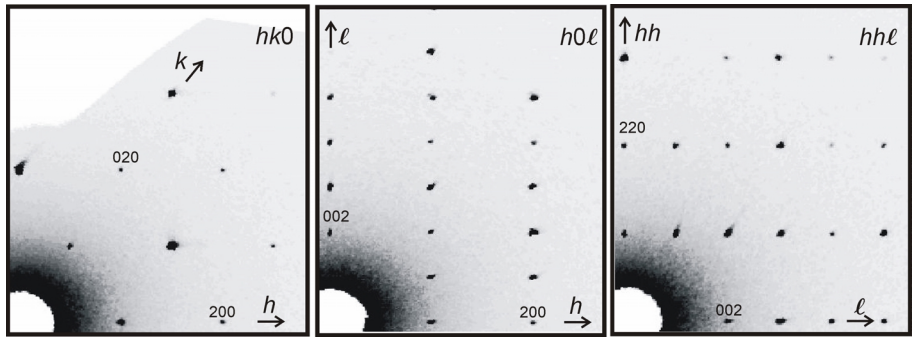

Fig. 3. Reconstructed reciprocal *hk*0, *h*0*l*, and *hhl* layers of $Ce_{2/3}Zn_2As_2$.

present cutouts of the reciprocal layers *hk*0, *h*0*l* and *hhl*. There is no hint for additional Bragg reflections or for diffuse scattering. Thus, on the scale of single crystal X-ray diffraction we observe a statistical distribution of the defects, *i.e.* the average structure of $Ce_{0.629}Zn_2As_2$.

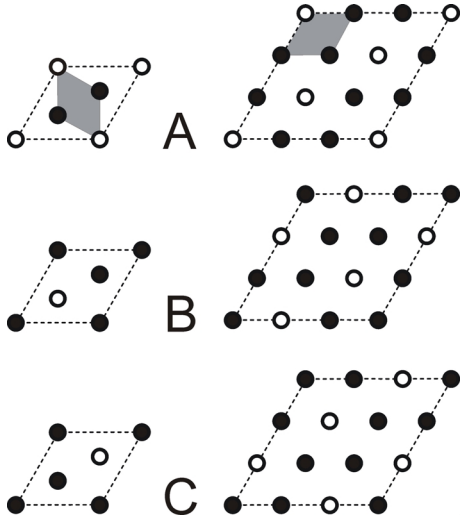

Fig. 4. Possible ordering variants of filled (filled circles) and vacant (open circles) rare earth sites in the arsenides $RE_{2/3}Zn_2As_2$. The subcell is marked by medium grey shading.

Two simple ordering variants of the close-packed layers are presented in Fig. 4. Keeping the composition of two filled *vs*. one unoccupied site, in the supercells $a\sqrt{3} \times a\sqrt{3}$ and $3a \times 3a$ one can keep trigonal symmetry. Permutation allows for three different layer types A, B and C for each superstructure cell. This is important for the stacking sequence along the *c* axis. A simple AA, BB or CC stacking of the ordered layers most likely will not occur, since in this way complete rows would remain empty along *c*, leading to a significant underbonding of the adjacent arsenic atoms. Thus at least every other layer needs to be shifted. One can then assume various rhombohedral or hexagonal stacking sequences for such compounds, but also severe stacking faults. We assume a high degree of short-range order in these arsenides, but a low degree of long-range order. The stacking faults are more or less random, similar to the sulfides $Gd_{2/3}Cu_2S_2$ [10] and $Er_{2/3}Cu_2S_2$ [11]. The latter compounds show substantial diffuse streaks in electron diffraction, as might also be expected for the arsenides studied herein.

The arrangement of 1/3 vacancies and 2/3 occupied atomic sites in the rare earth layers of the arsenides $RE_{2/3}Zn_2As_2$ as shown in Fig. 4 is similar to the arrangement of the transition metal and silicon atoms in the two-dimensionally close-packed layers of the structures of the transition metal disilicides TSi_2. Four of such layers (stacking sequence ABCD) are needed to complete a translation period perpendicular to the plane of the close-packed layers in orthorhombic $TiSi_2$, and three layers (stacking sequence ABC) in hexagonal $CrSi_2$, while two of such close-packed layers (stacking sequence AB) form a translation period in the tetragonal structure of $MoSi_2$ [26–30, and refs. therein]. Aside from the differing compositions with the separating $[Zn_2As_2]$ networks between the close-packed atomic sites, the structures of the potentially ordered rare earth zinc arsenides on the one hand and the structures of the transition metal disilicides on the other differ also in the way the close-packed layers are stacked on top of each other. In the expected ordered low-temperature modifications of the series $RE_{2/3}Zn_2As_2$ the vacant and occupied sites of the various layers must be situated exactly on top of each other when viewed along a projection along the (pseudo-)hexagonal axis of the layers because these expected ordered structures have the common hexagonal subcell reported here. In contrast, in the series of the disilicides the atomic sites of adjacent close-packed layers are shifted relative to each other when viewed in projections along a direction perpendicular to the planes of the layers.

Acknowledgement

This work was financially supported by the Deutsche Forschungsgemeinschaft through SPP 1458 *Hochtemperatursupraleitung in Eisenpnictiden*.

[1] Z. Ban, M. Sikirica, *Acta Crystallogr*. **1965**, *18*, 594.
[2] P. Villars, K. Cenzual, *Pearson's Crystal Data: Crystal Structure Database for Inorganic Compounds* (release 2009/10), ASM International®, Materials Park, Ohio, **2009**.
[3] P. Villars, L. D. Calvert, *Pearson's Handbook of Crystallographic Data for Intermetallic Phases*, 2nd ed., American Society for Metals, Materials Park, OH 44073, **1991**, and desk edition, **1997**.
[4] M. Rotter, M. Tegel, D. Johrendt, I. Schellenberg, W. Hermes, R. Pöttgen, *Phys. Rev. B* **2008**, *78*, 020503 (4 p).
[5] M. Rotter, M. Tegel, D. Johrendt, *Phys. Rev. Lett.* **2008**, *101*, 107006.
[6] E. I. Gladyshevskii, P. I. Krypyakevych, O. I. Bodak, *Ukr. Phys. J*. **1967**, *12*, 447.
[7] W. H. Zachariasen, *Acta Crystallogr*. **1948**, *1*, 265.

[8] a) A. Mahan, A. Mewis, *Z. Naturforsch.* **1983**, *38b*, 1041; b) P. Klüfers, A. Mewis, *Z. Kristallogr.* **1984**, *169*, 135; c) A. Artmann, A. Mewis, M. Roepke, G. Michels, *Z. Anorg. Allg. Chem.* **1996**, *622*, 679; d) R. Rühl, W. Jeitschko, *Mater. Res. Bull.* **1979**, *14*, 513; e) I. Schellenberg, M. Eul, W. Hermes, R. Pöttgen, *Z. Anorg. Allg. Chem.* **2010**, *636*, 85.
[9] P. E. R. Blanchard, S. S. Stoyko, R. G. Cavell, A. Mar, *J. Solid State Chem.* **2011**, *184*, 97.
[10] M. Onoda, X.-A. Chen, A. Sato, H. Wada, *J. Solid State Chem.* **2000**, *152*, 332.
[11] M. Guymont, A. Tomas, M. Julien-Pouzol, S. Jaulmes, M. Guittard, *Phys. Stat. Sol. A* **1990**, *121*, 21.
[12] A. T. Nientiedt, W. Jeitschko, *J. Solid State Chem.* **1999**, *142*, 266.
[13] A. T. Nientiedt, W. Jeitschko, *Inorg. Chem.* **1998**, *37*, 386.
[14] H. Lincke, R. Glaum, V. Dittrich, M. H. Möller, R. Pöttgen, *Z. Anorg. Allg. Chem.* **2009**, *635*, 936.
[15] P. Klüfers, H. Neumann, A. Mewis, H.-U. Schuster, *Z. Naturforsch.* **1980**, *35b*, 1317.
[16] G. Zwiener, H. Neumann, H.-U. Schuster, *Z. Naturforsch.* **1981**, *36b*, 1195.
[17] A. Nateprov, J. Cisowski, J. Heimann, I. Mirebeau, *J. Alloys Compd.* **1999**, *290*, 6.
[18] P. Klüfers, A. Mewis, *Z. Naturforsch.* **1977**, *32b*, 753.
[19] A. Mewis, *Z. Naturforsch.* **1980**, *35b*, 939.
[20] K. Yvon, W. Jeitschko, E. Parthé, *J. Appl. Crystallogr.* **1977**, *10*, 73.
[21] G. M. Sheldrick, SHELXL-97, Program for Crystal Structure Refinement, University of Göttingen, Göttingen (Germany) **1997**. See also: G. M. Sheldrick, *Acta Crystallogr.* **2008**, *A64*, 112.
[22] J. Emsley, *The Elements*, Oxford University Press, Oxford **1999**.
[23] A. Pietraszko, K. Lukaszewicz, *Bull. Acad. Polon. Sci., Ser. Sci. Chim.* **1976**, *24*, 459.
[24] H. Lincke, T. Nilges, R. Pöttgen, *Z. Anorg. Allg. Chem.* **2006**, *632*, 1804.
[25] H. Lincke, R. Glaum, V. Dittrich, M. Tegel, D. Johrendt, W. Hermes, M. H. Möller, T. Nilges, R. Pöttgen, *Z. Anorg. Allg. Chem.* **2008**, *634*, 1339.
[26] F. Laves, H. J. Wallbaum, *Z. Kristallogr.* **1939**, *A101*, 78.
[27] H. Nowotny, R. Kieffer, H. Schachner, *Monatsh. Chem.* **1952**, *83*, 1243.
[28] P. A. Beck, *Z. Kristallogr.* **1967**, *124*, 101
[29] W. Jeitschko, *Acta Crystallogr.* **1977**, *B33*, 2347.
[30] W. Jeitschko, R. Pöttgen, R.-D. Hoffmann in *Handbook of Ceramic Hard Materials*, (Ed.: R. Riedel), Vol. 1, Wiley-VCH, Weinheim, **2000**, pp. 3 – 40.